Global PM2.5 prediction and associated mortality to 2100 under different climate change scenarios

Journal:	*Environmental Science & Technology*
Manuscript ID	es-2022-04358z
Manuscript Type:	Article
Date Submitted by the Author:	24-Jun-2022
Complete List of Authors:	CHEN, Wanying; The Hong Kong University of Science and Technology, Division of Environment and Sustainability; Guangzhou HKUST Fok Ying Tung Research Institute, Atmospheric Research Center Lu, Xingcheng; The Hong Kong University of Science and Technology, Division of Environment and Sustainability; Guangzhou HKUST Fok Ying Tung Research Institute, Atmospheric Research Center; The Chinese University of Hong Kong, Department of Geography and Resource Management Yuan, Dehao; University of Maryland, Department of Computer Science Chen, Yiang; Hong Kong University of Science and Technology Li, Zhenning; The Hong Kong University of Science and Technology, Division of Environment and Sustainability Huang, Yeqi; The Hong Kong University of Science and Technology, Division of Environment and Sustainability Sun, Haochen; The Hong Kong University of Science and Technology, Department of Mathematics; The Hong Kong University of Science and Technology, Department of Computer Science and Engineering Fung, Jimmy; Hong Kong University of Science and Technology, Department of Mathematics

Global $PM_{2.5}$ prediction and associated mortality to 2100 under different climate change scenarios

Wanying Chen [1,2], Xingcheng Lu [3*], Dehao Yuan [4], Yiang Chen [1,2], Zhenning Li [1], Yeqi Huang [1], Haochen Sun [5,6], Jimmy C.H. Fung [1,2,6*]

[1] Division of Environment and Sustainability, the Hong Kong University of Science and Technology, Clear Water Bay, Hong Kong SAR, China

[2] Atmospheric Research Center, Guangzhou HKUST Fok Ying Tung Research Institute, Guangzhou, China

[3] Department of Geography and Resource Management, Chinese University of Hong Kong, Shatin, Hong Kong SAR, China

[4] Department of Computer Science, University of Maryland, College Park, Maryland, USA

[5] Department of Mathematics, the Hong Kong University of Science and Technology, Clear Water Bay, Hong Kong SAR, China

[6] Department of Computer Science and Engineering, the Hong Kong University of Science and Technology, Clear Water Bay, Hong Kong SAR, China

Correspondence to: Xingcheng Lu (xingchenglu2011@gmail.com), J.C.H. Fung (majfung@ust.hk).

Abstract

Ambient fine particulate matter ($PM_{2.5}$) can cause severe adverse health impacts in humans. Thus, reducing $PM_{2.5}$ exposure is an important public health focus. Meteorological and emissions factors, which considerably affect the $PM_{2.5}$ concentrations in air, vary significantly under different climate change scenarios. However, $PM_{2.5}$ concentrations and their associated disease burden under future climate scenarios are not well clarified. In this work, the global $PM_{2.5}$ concentrations from 2021 to 2100 were estimated by combining the U-Net convolutional neural network deep learning technique, reanalysis data, emissions data, and bias-corrected Coupled Model Intercomparison Project Phase 6 future climate scenario data. Based on the estimated $PM_{2.5}$ concentrations, the future premature mortality burden associated with $PM_{2.5}$ exposure was assessed using the Global Exposure Mortality Model. Ambient $PM_{2.5}$ exposure is expected to be highest in the SSP3-7.0 scenario and lowest in the SSP1-2.6 scenario in the major representative regions of the world. The global mortality rate (per 100,000 exposed population) associated with $PM_{2.5}$ under the four different scenarios (SSP1-2.6, SSP2-4.5, SSP3-7.0, and SSP5-8.5, ranging from 84.6 (95% CI: 59.6–107.0) to 150.0 (95% CI: 106.2–185.0)) at the end of this century is expected to be lower than the baseline (the 2010s, 161.1 (95% CI: 113.3–199.9)). Among all four scenarios, the sustainable development scenario (SSP1-2.6) results in the lowest $PM_{2.5}$ concentrations and the lowest premature mortality burden, which indicates that this is the pathway that countries should strive for. Our work helps to advance the scientific understanding of the global geo-climatic system and provides suggestions for scientists and policymakers.

Keywords: Climate change; Global; $PM_{2.5}$; Mortality; Deep learning

Synopsis: Future $PM_{2.5}$ pollution and its associated health burden have not been well clarified. In this study, a new set of global-scale, spatially explicit $PM_{2.5}$ concentration from 2021 to 2100 with a spatial resolution of 0.1°×0.1° was estimated, and associated $PM_{2.5}$ exposure and premature mortality burden was calculated.

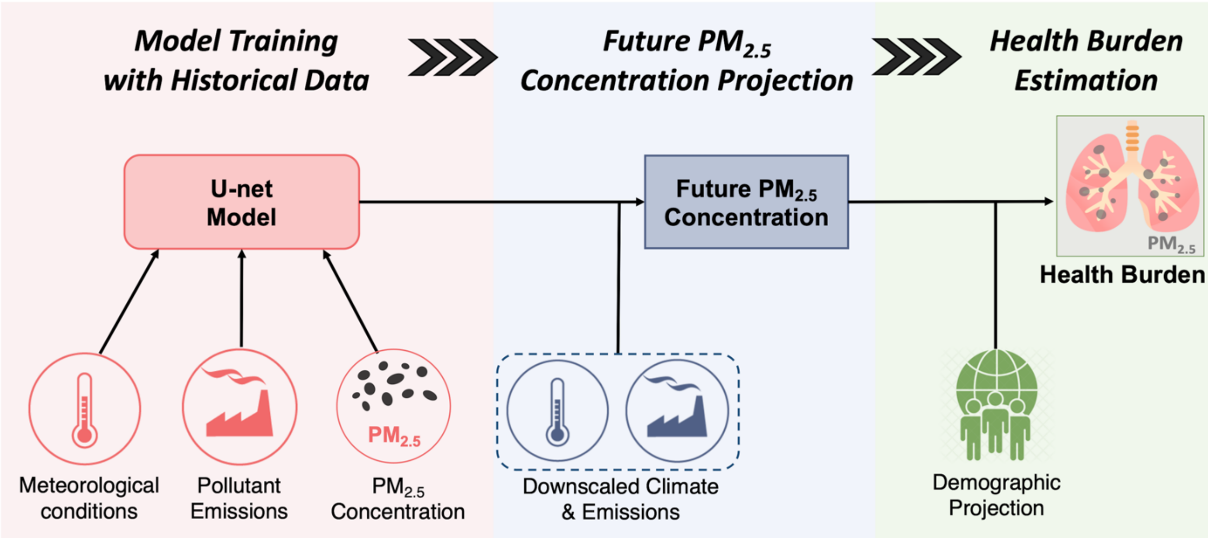

Graphic for Table of Contents (TOC)

1. Introduction

Ambient particulate matter ($PM_{2.5}$) poses a considerable global threat to human health. Exposure to outdoor $PM_{2.5}$ caused 4.14 million deaths in 2019, accounting for 62% of all global deaths attributable to air pollution estimated by the Global Burden of Disease Project.[1-4] Unmitigated climate change is projected to exacerbate inevitable challenges and threats to global air quality and increase its attributable adverse health impacts.[5-7] Therefore, it is necessary to understand how future climate change scenarios will influence surface $PM_{2.5}$ concentrations and propose appropriate climate mitigation measures.

Most studies[7, 8] on $PM_{2.5}$ concentration estimation under different climate scenarios have been based on the Coupled Model Intercomparison Project 5 (CMIP5) Representative Concentration Pathways scenarios. However, with the release of the CMIP6 simulation results, the Scenario Model Intercomparison Project provides new alternative scenarios that are intimately connected with societal concerns regarding climate change mitigation, adaptation, and impacts.[9, 10] Some studies have estimated future air quality based on CMIP6 climate projections;[11, 12] however, these studies either investigated the $PM_{2.5}$ exposure in only one country or region,[11-13] or the predicted periods were shorter than 50 years.[14, 15] Although future global-scale $PM_{2.5}$ simulations are available,[12, 16] the low model spatial resolution (e.g., 1.875° × 1.25°) prevents a clear understanding of how this pollutant will evolve over the next several decades and hampers reliable estimations of how this pollutant will influence human health in the future. As yet, no comprehensive study has estimated the global mortality burden associated with ambient $PM_{2.5}$ based on high-resolution (e.g., 0.1° × 0.1°) and bias-corrected future climate projections that incorporate demographic and emissions data. Such a study is urgently needed to understand how the $PM_{2.5}$ concentration and the associated health burden in each country will vary under different climate scenarios.

In this study, we estimated $PM_{2.5}$ exposure and its associated mortality burden over the 2021–2100 period under the SSP1-2.6[17], SSP2-4.5[18], SSP3-7.0,[19] and SSP5-8.5[20] scenarios (SSP: Shared Socioeconomic Pathway). The relationships between critical meteorological variables and $PM_{2.5}$ concentrations were constructed using a U-Net convolutional neural network[21] based on Modern-Era Retrospective Analysis for Research and Applications, version 2 (MERRA-2)[22], CMIP6 global emissions data,[23] and satellite-retrieved $PM_{2.5}$ data.[24] $PM_{2.5}$ exposure and the associated premature mortality over the 2021–2100 period were estimated based on the constructed relationships between the $PM_{2.5}$ concentrations, meteorological variables, and emissions, the high-resolution and bias-corrected CMIP6 future climate SSP scenario data (adjusted using the delta downscaling method), and future SSP demographic projections. Our work endeavored to elucidate how and through what pathways $PM_{2.5}$ exposure would influence the premature mortality burden in 184 countries and regions worldwide over the forthcoming 80 years, spanning the space of challenges to mitigation and adaptation to climate change, which can exhibit a more expansive and conscientious blueprint to air quality projection.

2. Methods

2.1. Data acquisition

2.1.1. Surface $PM_{2.5}$ data for training

High-resolution and highly accurate global surface $PM_{2.5}$ data are required to examine the relationships between $PM_{2.5}$ concentrations and meteorological and emissions conditions. Therefore, global surface $PM_{2.5}$ data at 0.1° × 0.1° combining AOD retrievals from the NASA MODIS, MISR, and SeaWIFS instrument, GEOS-Chem chemical transport model, and ground-based observations calibrated by geographically weighted regression were selected for the study.[24] Compared with previous global surface $PM_{2.5}$ concentration datasets,[25-27] this set of $PM_{2.5}$ values contained finer resolution data and compensated for missing or limited monthly measurements. This $PM_{2.5}$ dataset was highly consistent with collocated ground-based observations from monitoring networks $PM_{2.5}$ (R^2 = 0.84), with a root mean square error (RMSE) of 8.4 μg m^{-3}, and thus can accurately represent the surface $PM_{2.5}$ concentrations.

2.1.2. Meteorological and emissions data for model input

To train the deep learning model, the following monthly average meteorological data were taken from the MERRA-2 dataset:[28] surface temperature, wind speed, specific humidity, planetary boundary layer height, and sea level pressure; these parameters can strongly influence the $PM_{2.5}$ concentration.[29] Several studies have contrasted the MERRA-2 dataset with ground-based observations and other reanalysis datasets and have shown that the MERRA-2 data better represent the surface meteorological conditions.[22, 30-32] For example, when compared with the ground observation data from China, the RMSE, MB (mean bias), and R value for temperature were 3.62 K, −2.14 K, and 0.95, respectively.[33] These three statistical metrics for humidity were 5%, 0.63%, and 0.89.[34]

Primary $PM_{2.5}$ emissions data are not available in the CMIP6 dataset, we used the emissions of five pollutants (ammonia, nitrogen oxides, organic carbon, black carbon, and sulfur dioxide) as the emissions input for the deep learning model because these pollutants can have a marked influence on surface $PM_{2.5}$ concentrations.[35, 36] Based on existing global emission inventory, such as PKU-FUEL, primary $PM_{2.5}$ emission has high correlation with the

92 emissions of these five pollutants.[37, 38] Covering the 1750–2100 period (historical dataset: 1750–2014, future emissions dataset: 2015–2100), the CMIP6 gridded emissions dataset has previously been used for assessing air control policies and for comparing divergent emissions scenarios.[13, 39, 40]

95 The monthly MERRA-2 meteorological data and CMIP6 emissions data from 1998 to 2019 were input into the deep learning model for training and validation. Before training the deep learning model, all meteorological and emissions data were re-interpolated from their primary spatial resolutions into the same grid as the surface $PM_{2.5}$ data with a resolution of 0.1° × 0.1°. The bilinear interpolation technique was applied in this work, which has been widely used to interpolate climate data into different resolutions in previous studies.[41, 42]

100 **2.2. U-Net convolutional neural networks**

101 Tremendous advances in computer vision have led to convolutional neural networks (CNNs) being widely used for 2D data analysis.[43] We built a CNN-based U-Net framework to construct relationships between $PM_{2.5}$ concentrations and predictor variables.[21] First proposed for medical segmentation,[21] U-Net assumes that local information and global information are both essential, which is also apposite for $PM_{2.5}$ prediction. Equipped with flexible global aggregation blocks, U-Net can sufficiently consider non-local influences from other grid cells to local $PM_{2.5}$ concentration. In addition, multiple layers of U-Net CNNs make it possible to elucidate nonlinear relationships among critical meteorological variables, ambient pollutant emissions, and surface $PM_{2.5}$ concentrations; these relationships can be too complex to be delineated through traditional regression methods.[44-46]

109 All of the predictor variables (meteorological and emission data) and the $PM_{2.5}$ concentrations were treated as 2D images. The detailed architecture of our U-Net model, including the number of channels for each convolution layer, the size of the convolution kernel, the activation function of the convolution layer, and the image size are provided in Figure 1. The description of the U-Net model can be found in Text S1.

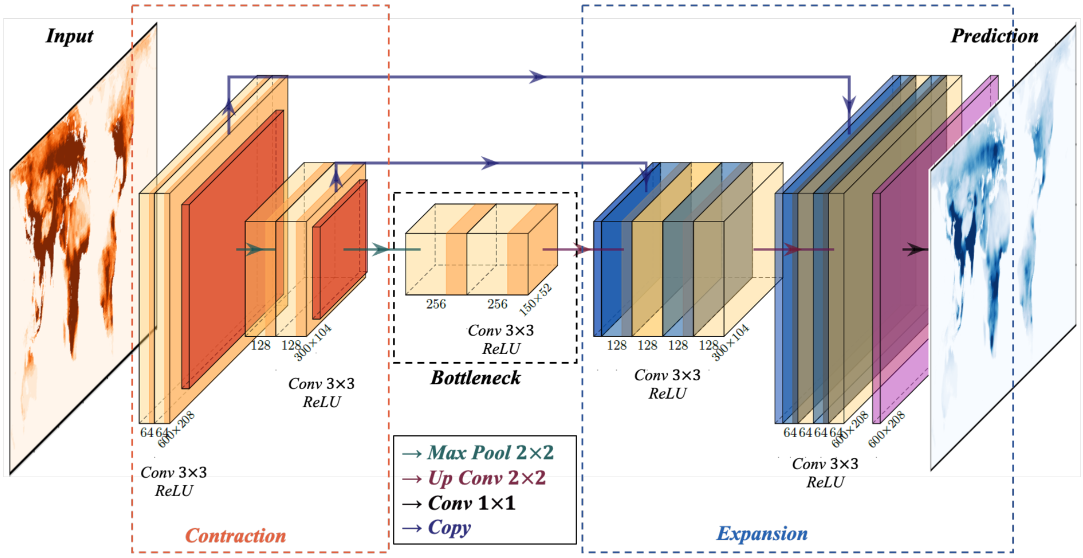

Figure 1. Architecture of the U-Net model

2.3. Future climate data under different Shared Socioeconomic Pathway (SSP) scenarios

The well-trained model was used to predict the 2021–2100 $PM_{2.5}$ concentrations using the meteorological variables from the CMIP6 future climate scenarios dataset. As shown in Table S1, historical simulations (1981–2010) and future projections (2021–2100) of global climate multiple-model ensemble results from 28 global climate models (GCMs) and four SSPs (SSP1-2.6, SSP2-4.5, SSP3-7.0, and SSP5-8.5) were utilized. The four SSPs are classified by socioeconomic, land use, and environmental development assumptions and represent conceivable future scenarios that capture distinctive climate mitigation and adaptation challenges. SSP1-2.6, SSP2-4.5, SSP3-7.0, and SSP5-8.5 represent low, medium, medium to high, and high radiative forcing by the end of the century, respectively.[47-49] Further information and the assumptions used in the future scenarios are provided in Eyring et al. (2016)[50] and Gidden et al. (2019).[51] The SSPs explored in this study cover a wide range of plausible socioeconomic trends for this century.

2.4. Bias correction and downscaling

Before being fed into the trained U-Net model, the meteorological variables from CMIP6 were corrected and downscaled to achieve reliable climate change impact metrics. To produce high-resolution and bias-corrected future climate information, we used the delta change (DC) method, which applies a change factor (i.e., delta) derived from GCMs to historical observations.[52, 53] Studies have found the DC method to be robust for downscaling climate data.[54, 55] Our implementation of the DC method was intended to correct the simulated climate data while providing results at high spatial resolution. The details of the DC method are described in the Text S2.

2.5. Mortality calculation

The Global Exposure Mortality Model (GEMM) proposed by Burnett et al. (2018)[56] was used as a hazard ratio model to estimate the premature mortality burden associated with $PM_{2.5}$ exposure. GEMM has relieved some of the contentious assumptions that are stipulated by other disease-specific hazard ratio models, such as the Integrated Exposure Response Model.[56] The detailed of the GEMM model are provided in the Text S3.

The baseline mortality rates for different countries in 2015 obtained from the Global Health Data Exchange data catalog were used for estimating premature mortality. The gridded population projections for all SSPs during 2021–2100 at a resolution of 1 km × 1 km are available from the Spatial Population Scenario database. This demographic projection dataset has been previously verified[57] and has been used to project heat-related excess mortality[58, 59] and to model future patterns of urbanization.[60] In this work, we calculated the $PM_{2.5}$-associated premature mortality in accordance with the projected population, but the baseline mortality rate was assumed to be that of 2015 owing to a lack of credible alternatives. Constant baseline mortality has been applied in other works that have projected the future environmental burdens of disease[61, 62].

3. Results

3.1. Performance evaluation

To verify that the well-trained U-Net model could generate accurate $PM_{2.5}$ concentration predictions, we validated the model performance from the spatial, scatter point, and statistical matrix perspectives. CMIP6 historical emissions data are available through 2014, while the data from 2015 to 2019 were from the CMIP6 future scenario emissions dataset. In the CMIP6 future scenario emissions dataset, the different scenarios (SSP1-2.6, SSP2-4.5, SSP3-7.0, and SSP5-8.5) have their own emissions datasets, but the differences are very limited throughout the 2015–2019 period. Because of this, we separated the verification by (1) implementing 8-fold cross-validation to verify the performance for the estimations from 1998 to 2014 and (2) inputting the future emissions datasets (2015–2019) of the four scenarios together with other independent variables into the well-trained model to output the $PM_{2.5}$ estimation for the comparison. For the 8-fold cross-validation, 15 years of data were used for training and 2 years of data were used for comparison in each fold.

Figure S2 shows a spatial comparison between the satellite-retrieved $PM_{2.5}$ data and the values predicted by the U-Net CNN using 8-fold validation. The results show that the model gave a well-fitted in the areas with both low (≤ 35 μg/m^3) and high (> 35 μg/m^3) $PM_{2.5}$ concentration. As demonstrated in Figures S3 and S4, the error between the simulated and target $PM_{2.5}$ concentrations for all grid cells was within ± 12 μg/m^3. The annual relative errors specific to each country were within ± 10%.

Figure 2 shows the scatter plots of the satellite-retrieved $PM_{2.5}$ concentrations and the 8-fold average predicted concentrations. The strong correlation coefficient (R, 0.987) was better than that of previous studies[63-65] and indicates that the model could accurately predict all of the 8-fold cross-validation data. The statistical evaluation metrics (A1–A5 in the supplemental material) shown in Table 1 were further used to verify the model performance. The NMB, NME, MB, and MAGE of the average 8-fold cross-validation were −0.0073 ± 0.0138, 0.2211 ± 0.0274, −0.0469 ± 0.0848 μg/m^3, and 1.3622 ± 0.1059 μg/m^3, respectively. The relatively small standard deviation of error indicates that our trained model has considerable stability. From these statistical matrix perspectives, the $PM_{2.5}$ concentrations estimated by our proposed deep learning model were also better than those of previous studies.[29, 66, 67] In addition to the comparison with the satellite-retrieved $PM_{2.5}$ data, we compared the annual model-predicted $PM_{2.5}$ concentrations with the monitor-based observations in China, the United States, and Europe because these regions have well-established ground-based observation networks (Table S2). The R values for China, the United States, and Europe were 0.91, 0.80, and 0.81, respectively. These results show that the $PM_{2.5}$ estimates from our method were also in general agreement with the ground-based observations in these regions.

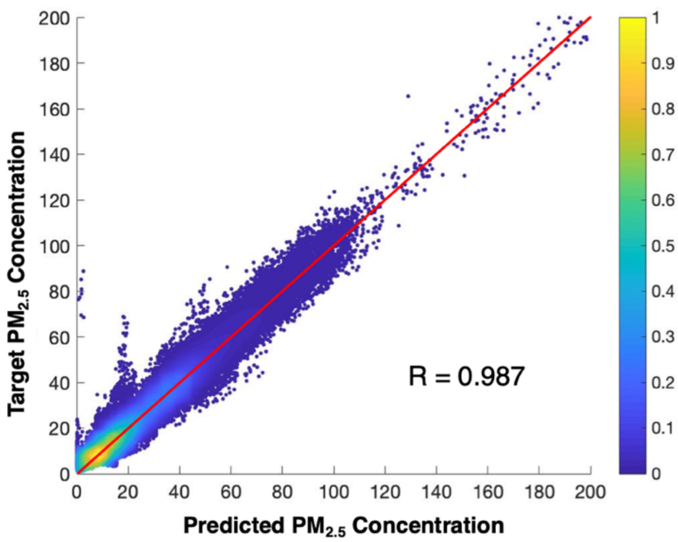

Figure 2. 8-fold cross-validation of the $PM_{2.5}$ concentrations predicted by the U-Net convolutional neural network model. The color represents the sample density.

Table 1. 8-fold cross-validation of U-Net convolutional neural network model performance

	NMB*	NME*	MB* ($\mu g/m^3$)	MAGE* ($\mu g/m^3$)	R
8-fold average	−0.0073	0.2211	−0.0469	1.3622	0.987
Standard error	0.0138	0.0274	0.0848	0.1059	0.010

***NMB:** normalized mean bias; **NME:** normalized mean error; **MB:** mean bias; **MAGE:** mean absolute gross error

As mentioned above, the CMIP6 emissions from 2015–2019 under the four SSP scenarios together with other input data were fed into the trained deep learning model to estimate the $PM_{2.5}$ concentrations for these 5 years, as shown in Table S3. The NMB ranged from 0.146 to 0.157 with an average of 0.148, the NME ranged from 0.338 to 0.341 with an average of 0.339, the MB ranged from 0.824 to 0.828 $\mu g/m^3$, and the MAGE ranged from 1.911 to 1.957 $\mu g/m^3$. These metrics indicate the good feasibility and generalizability of our model in predicting the $PM_{2.5}$ concentrations. In summary, the satisfactory performance indicated that the trained U-Net model was able to identify the relationships between $PM_{2.5}$ and the influencing factors, which demonstrates that this model could be used for future $PM_{2.5}$ pollution estimation in the 2021–2100 period under different climate scenarios.

3.2. Projection of future ambient $PM_{2.5}$ concentrations

The built U-Net deep learning model was used to project future $PM_{2.5}$ concentrations under the SSP1-2.6, SSP2-4.5, SSP3-7.0, and SSP5-8.5 scenarios. Changes in the downscaled multi-model ensembles of critical meteorological variables are shown in Figures S5–S9. The projected $PM_{2.5}$ concentrations were compared with the baseline concentration (the average $PM_{2.5}$ concentration from 2010 to 2019), as shown in Figure 3. The $PM_{2.5}$ decadal average concentrations for the different SSP scenarios are shown in Figures S10–S13.

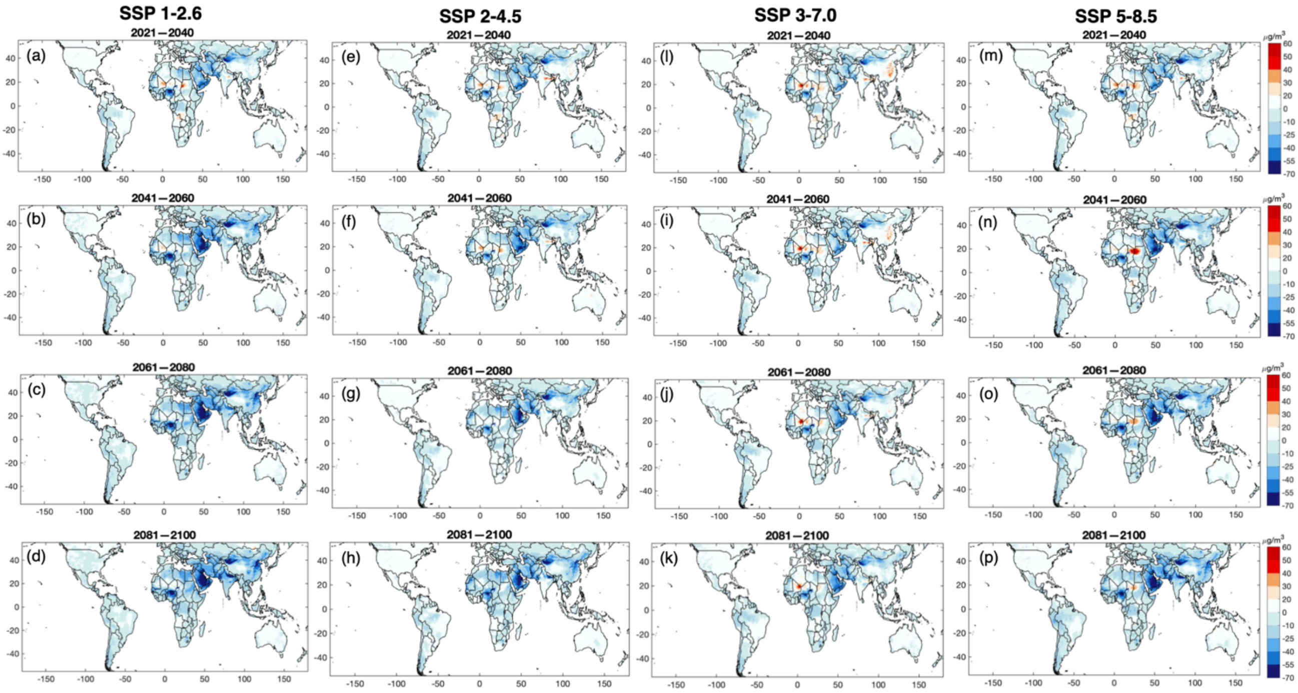

Figure 3. Spatial distribution of changes in projected global $PM_{2.5}$ concentrations relative to the baseline period (2010–2019) under different climate change scenarios.

Based on the deep learning model estimations, the $PM_{2.5}$ concentrations are projected to decrease in almost all regions in all scenarios; however, there are some notable differences among the projections. In SSP1-2.6, the projected $PM_{2.5}$ concentration will decrease consistently from 2030 to 2100. Among the investigated regions, the Middle East, Eastern China, and India will undergo the most significant decline in $PM_{2.5}$ concentrations under this scenario. SSP2-4.5 represents the middle range of plausible future pathways. In this scenario, although the furthest projection into the 2090s showed a decline compared with the baseline level (that of the 2010s), this reduction was much smaller than the corresponding changes under SSP1-2.6. The projections are different for SSP3-7.0, which assumes more pessimistic development strategies, such as less investment in the environment and health care and a fast-growing population.[17, 19, 68] This would lead to an apparent increase in $PM_{2.5}$ concentrations in Asia and Africa before the 2050s. After meeting economic development needs and implementing environmental control measures, the $PM_{2.5}$ concentrations would decrease to a level similar to the baseline period. In SSP5-8.5, fossil fuels are heavily relied on to achieve rapid economic growth. Thus, in the middle of the 21st century, climate change would considerably increase the $PM_{2.5}$ concentrations and cause considerable damage to human health in central Africa. Nevertheless, with the rapid development of society and pollution mitigation policies, the overall $PM_{2.5}$ concentrations will undergo a sharper reduction after the 2050s.

3.3. Projection of future ambient $PM_{2.5}$ exposure

Derived from the disproportionate spatial and temporal asymmetry under four SSP scenarios, the $PM_{2.5}$ exposure concentrations that coalesced with the future geographically demographic information can reveal the health intimidation to people from the future. Figures S14 and S15 show the demographic projections for the four SSPs scenarios for the world and for different regions, respectively.

Figure 4 shows the projected $PM_{2.5}$ exposure concentrations in several representative regions (North America, South America, Europe, Africa, the Middle East, Russia and Economies in Transition [EIT], Asia, and the rest of the world) under the various SSP scenarios. The region boundaries are shown in Figure S16. Overall, $PM_{2.5}$ exposure is highest in the SSP3-7.0 scenario and lowest in the SSP1-2.6 scenario for the major representative regions of the world, although the main drivers for the projected outcomes differ.

In Europe and North America, where $PM_{2.5}$ concentrations will be relatively low, the population distribution is the main determinant of $PM_{2.5}$ exposure. Space-weighted $PM_{2.5}$ concentrations will be lower in the SSP5-8.5 scenario owing to the stronger pollution control measures than in the "middle of the road" SSP2-4.5 scenario, but the population-weighted $PM_{2.5}$ concentrations in SSP5-8.5 will slightly exceed those of SSP2-4.5 and even surpass those of SSP3-7.0 after the 2060s. These trends will be caused by the higher birthrate in Europe and North America in SSP5-8.5 driven by economic optimism and international migration, leading to accelerated population growth in these two regions (Figures S15 and S17).[69] This implies that a greater share of the population will be concentrated in areas with higher levels of social development and education. Therefore, compared with SSP2-4.5, the SSP5-8.5 scenario will result in a higher population-weighted $PM_{2.5}$ exposure in North America and Europe after the 2060s.

In both Asia and Africa, $PM_{2.5}$ exposure will decline steadily over time, reaching −58.2% (−47.3%) and −52.5% (−32.0%) for Asia (Africa) by the end of the century under the SSP1-2.6 and SSP5-8.5 scenarios, respectively, compared with the baseline period. However, there will be no significant decline under the SSP3-7.0 scenario, and before the 2060s, the exposure levels will be even higher than in the baseline period. Two explanations can be offered for the persistently high exposure concentrations in Asia and Africa under the SSP3-7.0 scenario. The emissions and unfavorable meteorological factors will lead to increased $PM_{2.5}$ pollution under this scenario before the 2030s.

Meanwhile, population increase due to high fertility accompanied by slow urbanization in these regions will intensify the density of urban and rural settlement patterns, thereby increasing $PM_{2.5}$ exposure.[69]

We also estimated the proportion of the population that would be exposed to the previous and current Air Quality Guideline (AQG) values under future climate change scenarios. As shown in Figure S18, the trends in the population fraction exposed to the AQG values of 10 μg/m³ and 5 μg/m³ are similar for the four climate change scenarios, although there are considerable differences in the magnitude of the population fraction that would be exposed. By 2100, in the SSP1-2.6 scenario, 3.5% of the world's population will live in areas that have $PM_{2.5}$ concentrations lower than 5 μg/m³, which is well above the baseline population fraction of 2.0%. Compared with the other three scenarios, SSP1-2.6 would emerge victorious with tremendous benefits to global public health. Once SSP1-2.6 is not approachable, the other scenarios are comparable in terms of the proportion of the population exposed to the two AQG values.

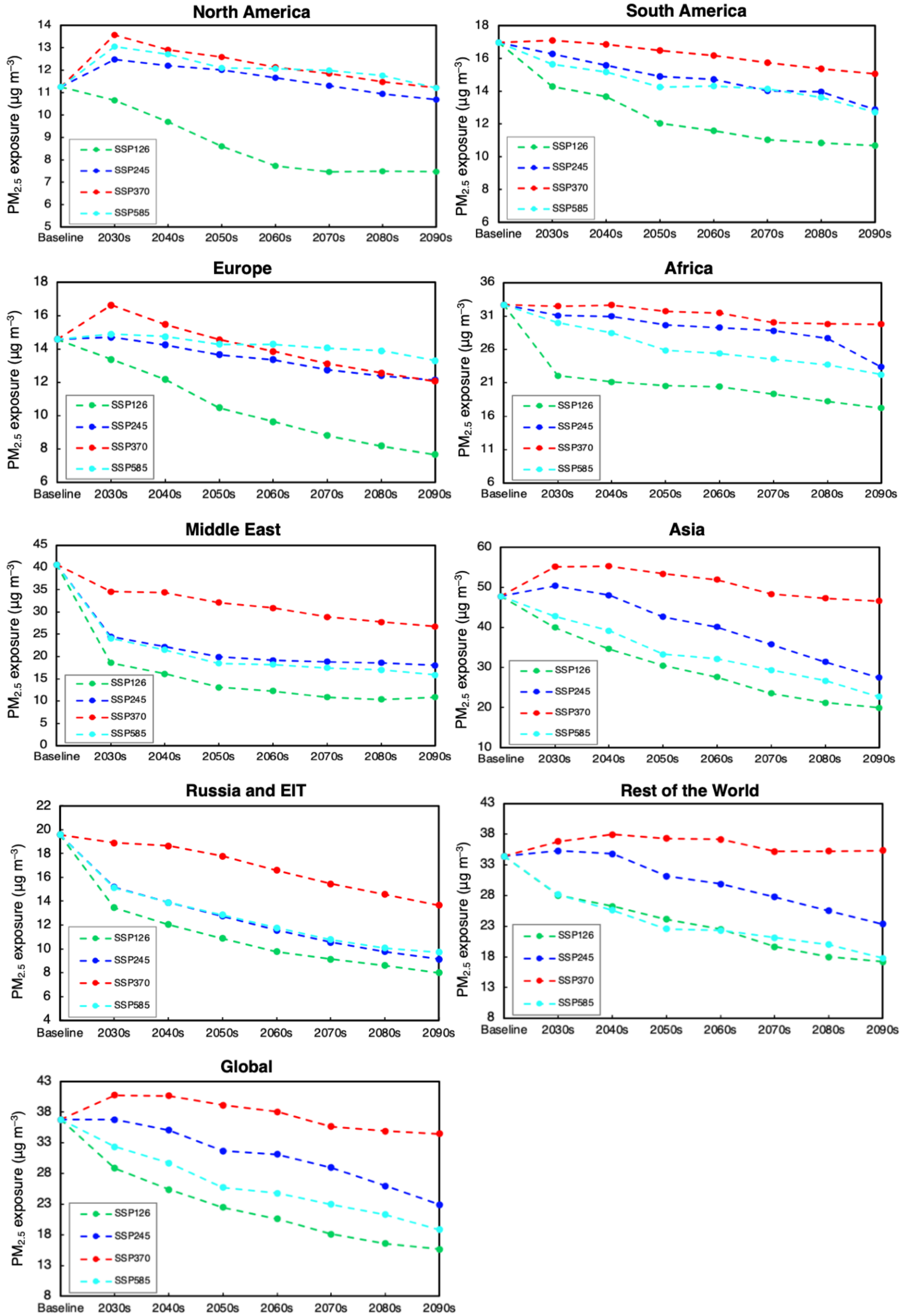

Figure 4. Projected ambient $PM_{2.5}$ exposure concentrations for 2030–2100 under different climate change scenarios.

3.4. Projection of premature mortality burden

The global premature mortality burden associated with future $PM_{2.5}$ concentrations under the different SSP scenarios was also analyzed. Figure 5 shows the $PM_{2.5}$-associated premature deaths for the baseline (2010–2019) and future (2030–2100) periods in several representative regions. The green growth and sustainable development assumptions in the SSP1-2.6 scenario would lead to a rapid reduction in air pollution emissions globally. Therefore, the number of $PM_{2.5}$-associated premature deaths worldwide would start to decline in the near future (2031–2040) before the population growth turning point (2071–2080). Given the middle-road development pattern of SSP2-4.5, premature deaths in this scenario would peak at 9,023,922 (95% CI: 6,352,113–11,236,028) in the 2060s and then steadily decline to 7,393,925 (95% CI: 5,202,070–9,290,539) in the final decade of the century, which is a less rapid decline than in the SSP1-2.6 scenario. SSP3-7.0 assumes weak pollution control in which the implementation of pollution mitigation measures is delayed and less ambitious in the long term. In this scenario, premature deaths would spike dramatically in all regions except North America, Europe, and Russia and would not decrease until the end of the century. The global number of $PM_{2.5}$-associated premature deaths would reach 11,148,502 (95% CI: 7,876,580–13,800,471) in 2091–2100, an increase of 63% from the baseline period. In the SSP5-8.5 scenario, which emphasizes technological progress and rapid economic growth through human capital development, environmental issues become a priority health concern, and ambitious air quality goals result in pollutant levels well below current levels in the medium to long term.[16, 70] Therefore, in SSP5-8.5, global premature deaths would peak at 8,508,685 (95% CI: 5,980,955–10,617,435) in the 2040s and then decline to 6,257,869 (95% CI: 4,410,176–7,886,851) in the second half of the 21st century as high-performance pollution control technologies are developed. This decrease would result in a smaller premature death burden than in the baseline period.

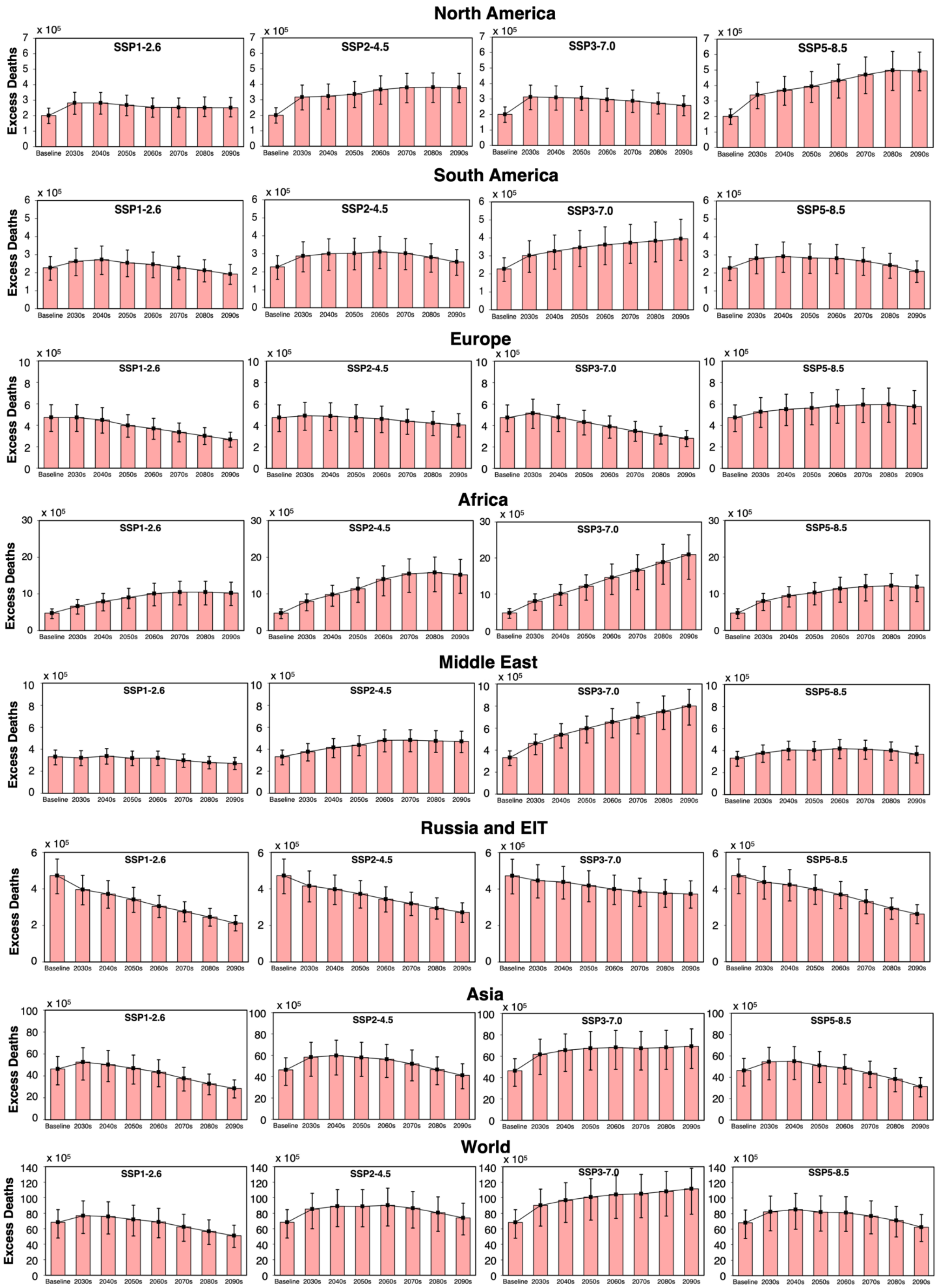

Figure 5. $PM_{2.5}$-associated premature deaths (> 25 years old) in different regions. The red bars represent the premature mortality rate, and the vertical black lines indicate the 95% empirical confidence intervals.

Because the size of the population will determine the absolute number of premature deaths, country-specific mortality rates per 100,000 people were used to describe the $PM_{2.5}$-associated mortality burden. Figure S19 shows the mortality rate per 100,000 people for 184 countries or districts. Overall, countries in North America, Western Europe, and Oceania will have the lowest mortality rates. The mortality rates in Eastern European countries (e.g., Ukraine and Serbia) will be the highest, followed by some countries in Asia, such as China and India.

3.5. Key factors that influence the premature mortality burden

Two sensitivity studies were conducted to explore how future population distributions and $PM_{2.5}$ concentrations would affect the burden of $PM_{2.5}$-associated premature mortality (Table S4). In the first (SA1) and second (SA2) sensitivity experiment, the population size and the $PM_{2.5}$ concentration was the same as that in 2010–2019, respectively.

When considering only the future demographic projections (i.e., demographic changes and changes in total population by age), the changes in the population distribution over the coming decades (2021–2040) will exacerbate the burden of premature deaths in all four scenarios, but the magnitude of the effect differs among the scenarios. These differences are reflected in the demographic assumptions about the birthrate, mortality, and migration.[71] SSP1-2.6 and SSP5-8.5 both envision a development path of increased investment in education and health, thereby accelerating the demographic transition.[69] Therefore, in these two scenarios, the demographic turning point in population decline will be reached earlier, in the medium term (2050s) (Fig. S13), after which the impact of demographics on the burden of premature mortality will gradually decrease.

In the second sensitivity experiment, we explore the effect of the $PM_{2.5}$ concentration on premature mortality assuming a constant future population distribution and size. Disease burden alleviation resulting from implementing air pollution control measures will become apparent in the near future under the SSP1-2.6 and SSP5-8.5 scenarios. SSP1-2.6 is the only scenario in which the effect of the $PM_{2.5}$ concentration will be greater than the effect of population size by the end of the century. Rapidly declining emissions would successfully offset the burden of premature mortality resulting from population growth by the end of the century. Under the SSP3-7.0 scenario, the planetary boundary layer height critically influences $PM_{2.5}$ dispersion, and it decreases in East Asia, South Asia, and eastern Africa (Figure S7). The decrease in the planetary boundary layer height will increase the $PM_{2.5}$ concentrations and therefore exacerbate the $PM_{2.5}$-associated mortality burden until the 2050s in these regions.

3.6. Implications and limitations

Global climate change is a significant challenge for society, and its impact on future air pollution is a critical perspective that requires quantitative assessment. Herein, a global $PM_{2.5}$ concentration dataset with a spatial resolution of 0.1° × 0.1° was estimated based on SSP scenarios. The results showed that the global $PM_{2.5}$ concentrations and the associated $PM_{2.5}$ exposure and premature mortality burden vary considerably under the four SSP scenarios. Among the scenarios, SSP1-2.6 would have the earliest inflection point for $PM_{2.5}$-associated premature deaths and the lowest mortality burden. This scenario presents an ideal target pathway that governments should strive to achieve.

This work has some limitations. First, satellite-retrieved $PM_{2.5}$ datasets were used as training targets, but according to the results in Table S2, there were discrepancies with the observational data obtained from ground measurements. Second, future climate, emission, and population projections harbor relatively large uncertainty, even if they have been calibrated against observed patterns of changes using historical data.[23, 69] Relative uncertainty generally increases over time because detailed spatial and temporal information is unavailable. Third, there are no generalizable and accurate findings that indicate how baseline mortality rates will change in the future. Therefore, in accordance with previous studies[72, 73] in the projection literature, we assumed that the nonlinear relationship between $PM_{2.5}$ concentrations and the baseline mortality rate would also be consistent. Fourth, the $PM_{2.5}$ projections derived in this study were based on several underlying assumptions. Primarily, in line with previous works,[72, 73] the relationships between $PM_{2.5}$ concentrations and meteorological conditions and precursor emissions explored in this study were assumed to be true for future climate and emissions scenarios. Finally, our predictions were based on the premise that the world is steadily developing, and our method cannot predict the effects of uncontrollable factors (such as war and strong earthquakes) on $PM_{2.5}$ and population distributions. Despite these limitations, this work helps quantify the extent to which climate change will influence the $PM_{2.5}$ concentrations worldwide. The results can contribute to the ongoing assessment of $PM_{2.5}$-associated exposure and vulnerability under different climate change scenarios, and governments can use this information to design useful strategies to reduce pollution.

Acknowledgment

The work described in this paper was supported by National Natural Science Foundation of China (Project No. 42007203), Guangzhou Scientific and Technological Planning Project (Project No. 202102021297), the Research

Grants Council of Hong Kong Government (Project No.16305921), the Environment and Conservation Fund (ECF 2020123), and a grant from the Research Grants Council of the Hong Kong Special Administrative Region, China (Project Nos. AoE/E-603/18 and T31-603/21-N).

Reference

1. Cohen, A. J.; Brauer, M.; Burnett, R.; Anderson, H. R.; Frostad, J.; Estep, K.; Balakrishnan, K.; Brunekreef, B.; Dandona, L.; Dandona, R., Estimates and 25-year trends of the global burden of disease attributable to ambient air pollution: an analysis of data from the Global Burden of Diseases Study 2015. *The Lancet* **2017,** *389*, (10082), 1907-1918.
2. Collaborators, G. R. F., Global, regional, and national comparative risk assessment of 79 behavioural, environmental and occupational, and metabolic risks or clusters of risks, 1990–2015: a systematic analysis for the Global Burden of Disease Study 2015. *Lancet (London, England)* **2016,** *388*, (10053), 1659.
3. Lim, S. S.; Vos, T.; Flaxman, A. D.; Danaei, G.; Shibuya, K.; Adair-Rohani, H.; AlMazroa, M. A.; Amann, M.; Anderson, H. R.; Andrews, K. G., A comparative risk assessment of burden of disease and injury attributable to 67 risk factors and risk factor clusters in 21 regions, 1990–2010: a systematic analysis for the Global Burden of Disease Study 2010. *The lancet* **2012,** *380*, (9859), 2224-2260.
4. Murray, C. J.; Aravkin, A. Y.; Zheng, P.; Abbafati, C.; Abbas, K. M.; Abbasi-Kangevari, M.; Abd-Allah, F.; Abdelalim, A.; Abdollahi, M.; Abdollahpour, I., Global burden of 87 risk factors in 204 countries and territories, 1990–2019: a systematic analysis for the Global Burden of Disease Study 2019. *The Lancet* **2020,** *396*, (10258), 1223-1249.
5. Costello, A.; Abbas, M.; Allen, A.; Ball, S.; Bell, S.; Bellamy, R.; Friel, S.; Groce, N.; Johnson, A.; Kett, M., Managing the health effects of climate change: lancet and University College London Institute for Global Health Commission. *The lancet* **2009,** *373*, (9676), 1693-1733.
6. Wang, H.-J.; Chen, H.-P., Understanding the recent trend of haze pollution in eastern China: roles of climate change. *Atmospheric Chemistry and Physics* **2016,** *16*, (6), 4205-4211.
7. Hong, C.; Zhang, Q.; Zhang, Y.; Davis, S. J.; Tong, D.; Zheng, Y.; Liu, Z.; Guan, D.; He, K.; Schellnhuber, H. J., Impacts of climate change on future air quality and human health in China. *Proceedings of the National Academy of Sciences* **2019,** *116*, (35), 17193-17200.
8. Chowdhury, S.; Dey, S.; Smith, K. R., Ambient PM2. 5 exposure and expected premature mortality to 2100 in India under climate change scenarios. *Nature communications* **2018,** *9*, (1), 1-10.
9. O'Neill, B. C.; Tebaldi, C.; Vuuren, D. P. v.; Eyring, V.; Friedlingstein, P.; Hurtt, G.; Knutti, R.; Kriegler, E.; Lamarque, J.-F.; Lowe, J., The scenario model intercomparison project (ScenarioMIP) for CMIP6. *Geoscientific Model Development* **2016,** *9*, (9), 3461-3482.
10. Gidden, M. J.; Riahi, K.; Smith, S. J.; Fujimori, S.; Luderer, G.; Kriegler, E.; Vuuren, D. P. v.; Berg, M. v. d.; Feng, L.; Klein, D., Global emissions pathways under different socioeconomic scenarios for use in CMIP6: a dataset of harmonized emissions trajectories through the end of the century. *Geoscientific model development* **2019,** *12*, (4), 1443-1475.
11. Shim, S.; Sung, H.; Kwon, S.; Kim, J.; Lee, J.; Sun, M.; Song, J.; Ha, J.; Byun, Y.; Kim, Y., Regional Features of Long-Term Exposure to PM2. 5 Air Quality over Asia under SSP Scenarios Based on CMIP6 Models. *International journal of environmental research and public health* **2021,** *18*, (13), 6817.
12. Turnock, S. T.; Allen, R. J.; Andrews, M.; Bauer, S. E.; Deushi, M.; Emmons, L.; Good, P.; Horowitz, L.; John, J. G.; Michou, M., Historical and future changes in air pollutants from CMIP6 models. *Atmospheric Chemistry and Physics* **2020,** *20*, (23), 14547-14579.
13. Cheng, J.; Tong, D.; Liu, Y.; Yu, S.; Yan, L.; Zheng, B.; Geng, G.; He, K.; Zhang, Q., Comparison of current and future PM2. 5 air quality in China under CMIP6 and DPEC emission scenarios. *Geophysical Research Letters* **2021,** *48*, (11), e2021GL093197.
14. Cheng, J.; Tong, D.; Zhang, Q.; Liu, Y.; Lei, Y.; Yan, G.; Yan, L.; Yu, S.; Cui, R. Y.; Clarke, L., Pathways of China's

PM2. 5 air quality 2015–2060 in the context of carbon neutrality. *National science review* **2021,** *8*, (12), nwab078.

15. Liu, S.; Xing, J.; Westervelt, D. M.; Liu, S.; Ding, D.; Fiore, A. M.; Kinney, P. L.; Zhang, Y.; He, M. Z.; Zhang, H., Role of emission controls in reducing the 2050 climate change penalty for PM2. 5 in China. *Science of the Total Environment* **2021,** *765*, 144338.

16. Rao, S.; Klimont, Z.; Smith, S. J.; Van Dingenen, R.; Dentener, F.; Bouwman, L.; Riahi, K.; Amann, M.; Bodirsky, B. L.; van Vuuren, D. P., Future air pollution in the Shared Socio-economic Pathways. *Global Environmental Change* **2017,** *42*, 346-358.

17. Van Vuuren, D. P.; Stehfest, E.; Gernaat, D. E.; Doelman, J. C.; Van den Berg, M.; Harmsen, M.; de Boer, H. S.; Bouwman, L. F.; Daioglou, V.; Edelenbosch, O. Y., Energy, land-use and greenhouse gas emissions trajectories under a green growth paradigm. *Global Environmental Change* **2017,** *42*, 237-250.

18. Thomson, A. M.; Calvin, K. V.; Smith, S. J.; Kyle, G. P.; Volke, A.; Patel, P.; Delgado-Arias, S.; Bond-Lamberty, B.; Wise, M. A.; Clarke, L. E., RCP4. 5: a pathway for stabilization of radiative forcing by 2100. *Climatic change* **2011,** *109*, (1), 77-94.

19. Fujimori, S.; Hasegawa, T.; Masui, T.; Takahashi, K.; Herran, D. S.; Dai, H.; Hijioka, Y.; Kainuma, M., SSP3: AIM implementation of shared socioeconomic pathways. *Global Environmental Change* **2017,** *42*, 268-283.

20. Riahi, K.; Rao, S.; Krey, V.; Cho, C.; Chirkov, V.; Fischer, G.; Kindermann, G.; Nakicenovic, N.; Rafaj, P., RCP 8.5—A scenario of comparatively high greenhouse gas emissions. *Climatic change* **2011,** *109*, (1), 33-57.

21. Ronneberger, O.; Fischer, P.; Brox, T. In *U-net: Convolutional networks for biomedical image segmentation*, International Conference on Medical image computing and computer-assisted intervention, 2015; Springer: 2015; pp 234-241.

22. Bosilovich, M. G., *MERRA-2: Initial evaluation of the climate*. National Aeronautics and Space Administration, Goddard Space Flight Center: 2015.

23. Feng, L.; Smith, S. J.; Braun, C.; Crippa, M.; Gidden, M. J.; Hoesly, R.; Klimont, Z.; Van Marle, M.; Van Den Berg, M.; Van Der Werf, G. R., The generation of gridded emissions data for CMIP6. *Geoscientific Model Development* **2020,** *13*, (2), 461-482.

24. van Donkelaar, A.; Hammer, M. S.; Bindle, L.; Brauer, M.; Brook, J. R.; Garay, M. J.; Hsu, N. C.; Kalashnikova, O. V.; Kahn, R. A.; Lee, C., Monthly global estimates of fine particulate matter and their uncertainty. *Environmental Science & Technology* **2021,** *55*, (22), 15287-15300.

25. Hammer, M. S.; van Donkelaar, A.; Li, C.; Lyapustin, A.; Sayer, A. M.; Hsu, N. C.; Levy, R. C.; Garay, M. J.; Kalashnikova, O. V.; Kahn, R. A., Global estimates and long-term trends of fine particulate matter concentrations (1998–2018). *Environmental Science & Technology* **2020,** *54*, (13), 7879-7890.

26. Van Donkelaar, A.; Martin, R. V.; Brauer, M.; Hsu, N. C.; Kahn, R. A.; Levy, R. C.; Lyapustin, A.; Sayer, A. M.; Winker, D. M., Global estimates of fine particulate matter using a combined geophysical-statistical method with information from satellites, models, and monitors. *Environmental science & technology* **2016,** *50*, (7), 3762-3772.

27. Van Donkelaar, A.; Martin, R. V.; Brauer, M.; Boys, B. L., Use of satellite observations for long-term exposure assessment of global concentrations of fine particulate matter. *Environmental health perspectives* **2015,** *123*, (2), 135-143.

28. Gelaro, R.; McCarty, W.; Suárez, M. J.; Todling, R.; Molod, A.; Takacs, L.; Randles, C. A.; Darmenov, A.; Bosilovich, M. G.; Reichle, R., The modern-era retrospective analysis for research and applications, version 2 (MERRA-2). *Journal of climate* **2017,** *30*, (14), 5419-5454.

29. Lu, X.; Yuan, D.; Chen, Y.; Fung, J. C., Impacts of urbanization and long-term meteorological variations on global PM2. 5 and its associated health burden. *Environmental Pollution* **2021,** *270*, 116003.

30. Theresa, N. M.; Sempewo, J. I.; Tumutungire, M. D.; Byakatonda, J., Performance evaluation of CFSR, MERRA-2

and TRMM3B42 data sets in simulating river discharge of data-scarce tropical catchments: a case study of Manafwa, Uganda. *Journal of Water and Climate Change* **2021**.

31. Huang, L.; Guo, L.; Liu, L.; Chen, H.; Chen, J.; Xie, S., Evaluation of the ZWD/ZTD values derived from MERRA-2 global reanalysis products using GNSS observations and radiosonde data. *Sensors* **2020,** *20*, (22), 6440.

32. Carvalho, D., An assessment of NASA's GMAO MERRA-2 reanalysis surface winds. *Journal of Climate* **2019,** *32*, (23), 8261-8281.

33. Wen, A.; Wu, X.; Zhu, X.; Hu, G.; Qiao, Y.; Wang, D.; Lou, P., Evaluation of Merra-2 Land Surface Temperature Dataset and its Application in Permafrost Mapping Over China. *Xiadong and Zhu, Xiaofan and li, ren and ni, jie and Hu, Guojie and Qiao, Yongping and zou, defu and chen, Jie and Wang, Dong and Lou, Peiqin, Evaluation of Merra-2 Land Surface Temperature Dataset and its Application in Permafrost Mapping Over China*.

34. Zhang, J.; Zhao, T.; Li, Z.; Li, C.; Li, Z.; Ying, K.; Shi, C.; Jiang, L.; Zhang, W., Evaluation of Surface Relative Humidity in China from the CRA-40 and Current Reanalyses. *Advances in Atmospheric Sciences* **2021,** *38*, (11), 1958-1976.

35. Hodan, W. M.; Barnard, W. R., Evaluating the contribution of PM2. 5 precursor gases and re-entrained road emissions to mobile source PM2. 5 particulate matter emissions. *MACTEC Federal Programs, Research Triangle Park, NC* **2004**.

36. Gao, M.; Carmichael, G. R.; Saide, P. E.; Lu, Z.; Yu, M.; Streets, D. G.; Wang, Z., Response of winter fine particulate matter concentrations to emission and meteorology changes in North China. *Atmospheric Chemistry and Physics* **2016,** *16*, (18), 11837-11851.

37. Meng, J.; Liu, J.; Xu, Y.; Guan, D.; Liu, Z.; Huang, Y.; Tao, S., Globalization and pollution: tele-connecting local primary PM2. 5 emissions to global consumption. *Proceedings of the Royal Society A: Mathematical, Physical and Engineering Sciences* **2016,** *472*, (2195), 20160380.

38. Huang, Y.; Shen, H.; Chen, H.; Wang, R.; Zhang, Y.; Su, S.; Chen, Y.; Lin, N.; Zhuo, S.; Zhong, Q., Quantification of global primary emissions of PM2. 5, PM10, and TSP from combustion and industrial process sources. *Environmental science & technology* **2014,** *48*, (23), 13834-13843.

39. Cheng, J.; Tong, D.; Liu, Y.; Bo, Y.; Zheng, B.; Geng, G.; He, K.; Zhang, Q., Air quality and health benefits of China's current and upcoming clean air policies. *Faraday Discussions* **2021,** *226*, 584-606.

40. Hsieh, I.-Y. L.; Chossière, G. P.; Gençer, E.; Chen, H.; Barrett, S.; Green, W. H., An Integrated Assessment of Emissions, Air Quality, and Public Health Impacts of China's Transition to Electric Vehicles. *Environmental Science & Technology* **2022**.

41. Almazroui, M.; Saeed, S.; Saeed, F.; Islam, M. N.; Ismail, M., Projections of precipitation and temperature over the South Asian countries in CMIP6. *Earth Systems and Environment* **2020,** *4*, (2), 297-320.

42. Almazroui, M.; Saeed, S.; Islam, M. N.; Khalid, M. S.; Alkhalaf, A. K.; Dambul, R., Assessment of uncertainties in projected temperature and precipitation over the Arabian Peninsula: a comparison between different categories of CMIP3 models. *Earth Systems and Environment* **2017,** *1*, (2), 1-21.

43. LeCun, Y.; Bottou, L.; Bengio, Y.; Haffner, P., Gradient-based learning applied to document recognition. *Proceedings of the IEEE* **1998,** *86*, (11), 2278-2324.

44. Rybarczyk, Y.; Zalakeviciute, R., Machine learning approaches for outdoor air quality modelling: A systematic review. *Applied Sciences* **2018,** *8*, (12), 2570.

45. Zhang, Y.; Bocquet, M.; Mallet, V.; Seigneur, C.; Baklanov, A., Real-time air quality forecasting, part I: History, techniques, and current status. *Atmospheric Environment* **2012,** *60*, 632-655.

46. Catalano, M.; Galatioto, F.; Bell, M.; Namdeo, A.; Bergantino, A. S., Improving the prediction of air pollution peak episodes generated by urban transport networks. *Environmental science & policy* **2016,** *60*, 69-83.

47. Meehl, G. A.; Moss, R.; Taylor, K. E.; Eyring, V.; Stouffer, R. J.; Bony, S.; Stevens, B., Climate model intercomparisons: Preparing for the next phase. *Eos, Transactions American Geophysical Union* **2014,** *95*, (9), 77-78.

48. O'Neill, B. C.; Kriegler, E.; Riahi, K.; Ebi, K. L.; Hallegatte, S.; Carter, T. R.; Mathur, R.; van Vuuren, D. P., A new scenario framework for climate change research: the concept of shared socioeconomic pathways. *Climatic change* **2014,** *122*, (3), 387-400.

49. Van Vuuren, D. P.; Kriegler, E.; O'Neill, B. C.; Ebi, K. L.; Riahi, K.; Carter, T. R.; Edmonds, J.; Hallegatte, S.; Kram, T.; Mathur, R., A new scenario framework for climate change research: scenario matrix architecture. *Climatic Change* **2014,** *122*, (3), 373-386.

50. Eyring, V.; Bony, S.; Meehl, G. A.; Senior, C. A.; Stevens, B.; Stouffer, R. J.; Taylor, K. E. J. G. M. D., Overview of the Coupled Model Intercomparison Project Phase 6 (CMIP6) experimental design and organization. **2016,** *9*, (5), 1937-1958.

51. Gidden, M. J.; Riahi, K.; Smith, S. J.; Fujimori, S.; Luderer, G.; Kriegler, E.; Vuuren, D. P. v.; Berg, M. v. d.; Feng, L.; Klein, D. J. G. m. d., Global emissions pathways under different socioeconomic scenarios for use in CMIP6: a dataset of harmonized emissions trajectories through the end of the century. **2019,** *12*, (4), 1443-1475.

52. Ramírez Villegas, J.; Jarvis, A., Downscaling global circulation model outputs: the delta method decision and policy analysis Working Paper No. 1. **2010**.

53. Hay, L. E.; Wilby, R. L.; Leavesley, G. H. J. J. J. o. t. A. W. R. A., A comparison of delta change and downscaled GCM scenarios for three mountainous basins in the United States 1. **2000,** *36*, (2), 387-397.

54. Navarro-Racines, C.; Tarapues, J.; Thornton, P.; Jarvis, A.; Ramirez-Villegas, J. J. S. d., High-resolution and bias-corrected CMIP5 projections for climate change impact assessments. **2020,** *7*, (1), 1-14.

55. Hawkins, E.; Osborne, T. M.; Ho, C. K.; Challinor, A. J. J. A.; meteorology, f., Calibration and bias correction of climate projections for crop modelling: an idealised case study over Europe. **2013,** *170*, 19-31.

56. Burnett, R.; Chen, H.; Szyszkowicz, M.; Fann, N.; Hubbell, B.; Pope, C. A.; Apte, J. S.; Brauer, M.; Cohen, A.; Weichenthal, S. J. P. o. t. N. A. o. S., Global estimates of mortality associated with long-term exposure to outdoor fine particulate matter. **2018,** *115*, (38), 9592-9597.

57. Gao, J., Downscaling global spatial population projections from 1/8-degree to 1-km grid cells. *National Center for Atmospheric Research, Boulder, CO, USA* **2017,** *1105*.

58. Yang, J.; Zhou, M.; Ren, Z.; Li, M.; Wang, B.; Liu, D. L.; Ou, C.-Q.; Yin, P.; Sun, J.; Tong, S., Projecting heat-related excess mortality under climate change scenarios in China. *Nature communications* **2021,** *12*, (1), 1-11.

59. Rohat, G.; Wilhelmi, O.; Flacke, J.; Monaghan, A.; Gao, J.; Dao, H.; van Maarseveen, M., Characterizing the role of socioeconomic pathways in shaping future urban heat-related challenges. *Science of the total environment* **2019,** *695*, 133941.

60. Luo, C.; Posen, I. D.; Hoornweg, D.; MacLean, H. L., Modelling future patterns of urbanization, residential energy use and greenhouse gas emissions in Dar es Salaam with the Shared Socio-Economic Pathways. *Journal of Cleaner Production* **2020,** *254*, 119998.

61. Wang, Q.; Wang, J.; Zhou, J.; Ban, J.; Li, T., Estimation of PM2· 5-associated disease burden in China in 2020 and 2030 using population and air quality scenarios: a modelling study. *The Lancet Planetary Health* **2019,** *3*, (2), e71-e80.

62. Ingole, V.; Dimitrova, A.; Sampedro, J.; Sacoor, C.; Acacio, S.; Juvekar, S.; Roy, S.; Moraga, P.; Basagaña, X.; Ballester, J., Local mortality impacts due to future air pollution under climate change scenarios. *Science of the Total Environment* **2022,** *823*, 153832.

63. Park, Y.; Kwon, B.; Heo, J.; Hu, X.; Liu, Y.; Moon, T., Estimating PM2. 5 concentration of the conterminous United States via interpretable convolutional neural networks. *Environmental Pollution* **2020,** *256*, 113395.

64. Zheng, T.; Bergin, M. H.; Hu, S.; Miller, J.; Carlson, D. E., Estimating ground-level PM2. 5 using micro-satellite images by a convolutional neural network and random forest approach. *Atmospheric Environment* **2020,** *230*, 117451.

65. Li, S.; Xie, G.; Ren, J.; Guo, L.; Yang, Y.; Xu, X., Urban pm2. 5 concentration prediction via attention-based cnn–lstm. *Applied Sciences* **2020,** *10*, (6), 1953.

66. Xiao, F.; Yang, M.; Fan, H.; Fan, G.; Al-Qaness, M. A., An improved deep learning model for predicting daily PM2. 5 concentration. *Scientific reports* **2020,** *10*, (1), 1-11.

67. Yan, X.; Zang, Z.; Luo, N.; Jiang, Y.; Li, Z., New interpretable deep learning model to monitor real-time PM2. 5 concentrations from satellite data. *Environment International* **2020,** *144*, 106060.

68. Riahi, K.; Van Vuuren, D. P.; Kriegler, E.; Edmonds, J.; O'neill, B. C.; Fujimori, S.; Bauer, N.; Calvin, K.; Dellink, R.; Fricko, O., The shared socioeconomic pathways and their energy, land use, and greenhouse gas emissions implications: an overview. *Global environmental change* **2017,** *42*, 153-168.

69. Jones, B.; O'Neill, B. C., Spatially explicit global population scenarios consistent with the Shared Socioeconomic Pathways. *Environmental Research Letters* **2016,** *11*, (8), 084003.

70. Kriegler, E.; Bauer, N.; Popp, A.; Humpenöder, F.; Leimbach, M.; JS, B. L.; Bodirsky, B.; Hilaire, J.; Klein, D.; Mouratiadou, I., Fossil-fueled development (SSP5): an emission, energy and resource intensive reference scenario for the 21 st century. *Global Environ. Change* **2016**.

71. Samir, K.; Lutz, W., The human core of the shared socioeconomic pathways: Population scenarios by age, sex and level of education for all countries to 2100. *Global Environmental Change* **2017,** *42*, 181-192.

72. Liu, S.; Xing, J.; Wang, S.; Ding, D.; Cui, Y.; Hao, J., Health benefits of emission reduction under 1.5 C pathways far outweigh climate-related variations in China. *Environmental Science & Technology* **2021,** *55*, (16), 10957-10966.

73. Aleluia Reis, L.; Drouet, L.; Van Dingenen, R.; Emmerling, J., Future global air quality indices under different socioeconomic and climate assumptions. *Sustainability* **2018,** *10*, (10), 3645.